COMPARATIVE BAND STRUCTURE STUDY OF $SrTiO_3$ PEROVSKITE ON BULK AND LAYERED PHASES.

Submitted in partial fulfillment of the requirements for the award of

MASTER OF SCIENCE DEGREE IN PHYSICS

By

NIVETHA B

(40590003)

DEPARTMENT OF PHYSICS

SCHOOL OF SCIENCE AND HUMANITIES

SATHYABAMA

INSTITUTE OF SCIENCE TECHNOLOGY

(DEEMED TO BE UNIVERSITY)

Accredited with Grade "A" by NAAC

JEPPIAAR NAGAR, RAJIV GANDHI SALAI, CHENNAI - 600 119 APRIL -

2022

SATHYABAMA
INSTITUTE OF SCIENCE AND TECHNOLOGY
(DEEMED TO BE UNIVERSITY)
Accredited "A" Grade by NAAC | 12B Status by UGC | Approved by AICTE
www.sathyabama.ac.in

DEPARTMENT OF PHYSICS

BONAFIDE CERTIFICATE

This is to certify that this Project Report is the bonafide work of NIVETHA B (40590003) who carried out the project entitled **"COMPARATIVE BAND STRUCTURE STUDY OF $SrTiO_3$ PEROVSKITE ON BULK AND LAYERED PHASES"** under my supervision from NOV 2021 to APR 2022.

Internal Guide
(Dr.D.S.JAYALAKSHMI)

External Guide

Head of the Department
(Dr. S. RAVICHANDRAN)

Submitted for Viva-voce Examination held on

Internal Examiner **External Examiner**

DECLARATION

I NIVETHA B (Reg.No 40590003) hereby declare that the Project Report entitled on **"COMPARATIVE BAND STRUCTURE STUDY OF $SrTiO_3$ PEROVSKITE ON BULK AND LAYERED PHASES."** done by me under the guidance of **Dr.D.S. JAYALAKSHMI, ASST. PROFESSOR, DEPARTMENT OF PHYSICS** at SATHYABAMA INSTITUTE OF SCIENCE AND TECHNOLOGY, CHENNAI is submitted in partial fulfillment of the requirements for the award of Master of Science degree in Physics.

DATE:

PLACE: **SIGNATURE OF THE CANDIDATE**

ACKNOWLEDGEMENT

I am pleased to acknowledge my sincere thanks to the Board of Management of **SATHYABAMA** for their kind encouragement in doing this project and for completing it successfully. I am grateful to them.

I convey my thanks to the Dean, School of Science and Humanities and **Dr. S. RAVICHANDRAN,** Head of the Department, Dept. of Physics for providing me necessary support and details at the right time during the progressive reviews.

I would like to express my sincere and deep sense of gratitude to my Project Guide **Dr.D.S.JAYALAKSHMI** for her valuable guidance, suggestions and constant encouragement that paved way for the successful completion of my project work.

I wish to express my thanks to all Teaching and Non-teaching staff members of the Department of Physics who were helpful in anyways for the completion of the project.

NIVETHA B

ABSTRACT

A computational investigation over structural and electronic properties of perovskite compound namely $SrTiO_3$ using WIEN2K code by means of Full-potential (FP) Linearized Augmented Plane Wave (LAPW) method using DFT (Density Functional Theory) have been analyzed. In order to acquire a reasonable description of the structural, electronic, optical and thermal properties of the bulk and layered phases of perovskite compound $SrTiO_3$ have been computed. Further on this study we made surface structure of this compound by creating a supercell with various thickness of layer and compared the properties with bulk $SrTiO_3$. The surfaces of $SrTiO_3$ for varying thicknesses have been constructed using the Struct editor program implemented in the WIEN2k code. The structural parameters viz., lattice constant, bond length, bond angles, the electronic parameters such as band gap, DoS, band structure and optical fundamental constants like dielectric function, optical conductivity refraction and reflectivity, thermal properties such as Debye temperature, entropy, gibbs free energy with minimized energy (stabled / optimized state) have been computed and results agree well with the experimental studies and are similar to the compound used as reference which has been previously studied. The $SrTiO_3$ bulk and layered surface exhibit a direct band gap located at the Γ symmetry point of the Brillouin zone. These materials are favorable for opto-electronic devices.

TABLE OF CONTENTS

LIST OF TABLES

LIST OF FIGURES

LIST OF SYMBOLS AND ABBREVIATIONS

E_F - Fermi energy

F_L - Fermi level

$F_{HK}[\rho]$ - Hohenberg Kohn density

functional $N(E_F)$ - DOS Fermi level

n(r) - electron density

BZ - Brillouine Zone

DFT - Density Functional Theory

DOS - Density of states

FP-(L)APW - Full Potential - (Linearized) Augmented Plane

Wave GGA - Generalized gradient Approximation

GUI - Graphical User Interface

LDA - Local Density

Approximation LMTO - Linear Muffin

Tin Orbital OPW - Orthogonalized

Plane Wave RMT - Radius of Muffin Tin

spheres

EPM - Empirical Pseudo potential Method

E_G - Band gap

CHAPTER 1

1. Introduction

Understanding the nature of the material to the current hypothetical compound is critical for reducing the probability of experiment error. Computer stimulation helps in the study of complex materials containing many electrons and serves as a significant component in the process of analyzing and explaining intricate levels or rationally planning future experiments. In comparison to the previous trial and error process of improving a material by synthesizing, characterizing, and functional analyzing, the stimulation method is more efficient. Quantum mechanics determines the electronic structure of a system, which is responsible for aspects like relative stability, chemical bonding, atom relaxation, phase transitions, electrical, mechanical, and magnetic behavior, among others (Schwarz K et al 2002). Density functional theory is a well-known method for calculating the electrical characteristics of solids (DFT). DFT is a well-known computational quantum mechanical modelling method for many body systems, such as atoms, molecules, and condensed phases, in physics, chemistry, and material science. It treats both exchange and correlation and is based on electron density rather than wave function (Hartree Fock). Our compounds are investigated using the WIEN2K computer code, which is one of many accessible.

The interatomic distance is crucial for the majority of solid interactions. Pressure modifies the structure and electrical characteristics of a material without adding any chemical complexity and keeping physical complexity to a minimum. In recent years, high pressure techniques have been widely employed to investigate the physical state of solids, to produce new ground states in solids, to test theoretical models, and to assist the development of new theories. In the last half-century, for example, more naturally non-superconducting elements have been converted to superconductors through the application of pressure than natively superconducting elements. As a result, high-pressure systems may be studied computationally.

1.1 DENSITY FUNCTIONAL THEORY

Density functional theory (DFT) is a prominent method of calculating electronic structure. DFT has been the most successful and widely used method in condensed-matter physics, computational physics, and quantum chemistry to describe properties of condensed matter systems, which include not only standard bulk materials but also complex materials such as molecules, proteins, interfaces, and nanoparticles. A functional is a characteristic's function. The functional in DFT is the electron density, which is a property of area and time. Unlike the Hartree-Fock principle, which works directly with the many-body wavefunction, DFT uses electron density as the fundamental feature. The calculation is accelerated up by utilizing the electron density significantly. Unlike the many-body electronic wavefunction, which is a function of 3N variables (the coordinates of all N atoms in the system), the electron density is a function of only three variables: x, y, and z. Of course, performing a historical calculation quickly isn't always sufficient; we must also verify that we can derive something significant from it. It was Hohenburg and Kohn who stated a theory stating that electron density is extremely advantageous. The Hohenburg-Kohn theorem states that a machine's density determines all of its floor-country residences. The entire ground country strength of a many-electron device is a function of density in this example. So, if we purposefully recognize the electron density, we recognise the entire energy of our machine. DFT's basic idea is to explain a many-body interacting device by its particle density rather than its many-body wave function.

Its relevance is that it reduces the N body system's 3N degrees of freedom to only 3 spatial coordinates thanks to its particle density. It is based on the well-known Hohenberg-Kohn (HK) theorem, which states that all of a gadget's features can be considered to be unique functions of its ground state density. With the Born-Oppenheimer (BO) approximation and the Kohn-Sham (KS) equation, approximations for the so-called exchange-correlation (XC) potential, which describes the effects of the Pauli principle and the Coulomb capability beyond a pure electrostatic interaction of the electrons, practical accurate DFT calculations have been made possible.

Because calculating the exact XC potential (by solving the numerous-body problem exactly) is impossible, a common approximation is the so-called local density approximation (LDA), which locally substitutes an inhomogeneous system's XC energy density through that of a homogeneous electron gas evaluated at the local density. In many cases, the results of DFT calculations for condensed-matter systems coincided pretty well with experimental data, particularly since the 1990s, when better estimates for the XC energy functional were available. In addition, compared to established methods based on the complex many-electron wave function, such as Hartree-Fock theory and its descendants, the computational costs were comparatively cheap. Despite advances in DFT, utilizing it to accurately represent intermolecular interactions, charge transfer excitations, transition states, international potential energy surfaces, and other strongly correlated systems, as well as computing the band gap of particular semiconductors, is still a challenge.

There are several different ways for calculating independent particle electronic states in solids using boundary conditions. They can be classified into three groups: Plane wave codes include ESPRESSO, ABINIT, VASP, and others; localized atomic orbitals include CRYSTAL, SIESTA, and others; and augmented plane wave codes include LMTO, FLEUR, and IEN2K. The WIEN2K code employs the full potential (linearized) augmented plane wave (LAPW)+ local orbitals (LO) method.

1.2 OVERVIEW OF DFT

Ab initio (from first principles) DFT calculations in computational materials science allow for the prediction and calculation of material behaviour based on quantum mechanical considerations without the use of higher order parameters such as fundamental materials properties. The electronic structure is analysed using a potential acting on the system's electrons in modern DFT techniques. This DFT potential is made up of an external potential Vext that is purely determined by the system's structure and elemental composition, and an effective potential V_{eff} that represents interelectronic interactions. As a result, an issue involving a typical supercell of a material with n electrons can be analysed using a set of n one-electron Schrödinger type equations,

commonly known as Kohn-Sham equations.

1.3 BASIS FUNCTION

In order to efficiently describe the electronic wave function when solving Kohn-Sham equations numerically, we must use a set of basis functions in addition to the exchange correlation potential and full potential. By expanding the basis sets of atomic orbitals, first-principles computations for electronic structure are used.

1.4 LINEARIZED AUGMENTED PLANE WAVE (LAPW) METHOD

The weakly bound electrons (e.g., valence electrons) in the LAPW approach are well described by PW, which are the solutions to the Hamiltonian with a zero potential. A core electron, on the other hand, "feels" practically only the nucleus to which it is bound, and hence it is well represented by spherical harmonics (solutions for a single free atom). By placing a muffin-tin (MT) sphere on each atom, the LAPW method integrates these two basis sets. The interstitial region is the remainder of the space.

Electrons in an atom can be classified into two categories based on whether or not they participate in chemical bonding with other atoms. Core electrons are one form of electron that is highly attached to its nucleus and hence completely localised in the MT sphere. The associated states are referred to as core states. Valence electrons are the other type of electrons that leak out of the MT sphere and bind with other atoms. However, for many elements, the electrons cannot be separated in this manner. Some states are referred to as semi-core states since they are neither confined in the core states nor lie in the valence states. They have the same angular quantum number I as valence states but have a smaller primary quantum number n. The LAPW approach treats semi-core states by introducing local orbits. Local orbitals are independent of k and G, yet they solely belong to one atom and have a distinct character. They are named local because they are restricted to the muffin-tin spheres and hence have zero interstitial value.

Because the basis allows for substantial variational freedom, the LAPW approach can be easily extended to non-spherical muffin-tin potentials. The full-potential linearized augmented plane wave approach follows.

1.5 FULL - POTENTIAL LINEARIZED AUGMENTED PLANE WAVE (FP-LAPW) METHOD

The linearized augmented plane wave (LAPW) approach is one of the most accurate methods for calculating crystal electrical structure. For the treatment of exchange and correlation, it is based on density functional theory and employs techniques such as the local spin density approximation (LSDA). The potential is approximated to be spherical inside the muffin tins, whilst the potential is ready to be constant in the interstitial zone. It is a method for simulating the electrical characteristics of materials using DFT. Because of the high precession, it is widely acknowledged that it provides a density-functional solution to the problem. The shape of the charge density, the one-electron potential, and the wavefunction are all taken into account with great accuracy.

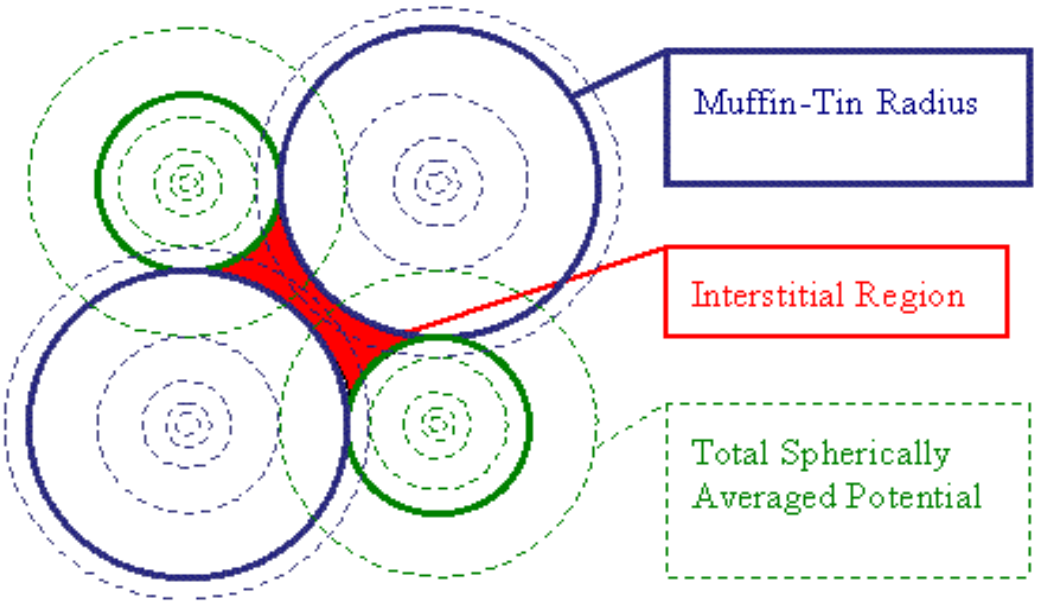

Fig.1.1. The unit cell divided into muffin-tin region and interstitial region

The FLAPW technique is an all-electron algorithm that is applicable to all atoms in the periodic table, particularly transition metals and rare earths, as well as multi-atomic systems with compact and open structures. Because of the method's all-electronic character, magnetism is properly safeguarded, and nuclear parameters such as isomer shift, hyperfine field, electric powered field gradient (EFG), and core level shift are frequently determined. Open structures such as surfaces, clusters, organic and inorganic molecules, and wires can also be addressed without difficulty. The capacity to calculate atomic forces exerted on atoms paves the way for structural optimization.

This method has been successfully applied to study structural phase transitions of certain semiconductors, which will increase the number of plane waves in the basis set, in order to lower the structural properties of systems accurately. This method has been used successfully to analyse structural phase transitions of certain semiconductors, which will increase the number of plane waves in the basis set in order to precisely lower the structural properties of systems. In this method, the shape of the charge density is taken into consideration with high precision; the unit cell is separated into two parts I Muffin tin radius (ii) interstitial region (iii) total spherically averaged potential.

The potential and charge density are extended into lattice harmonics inside each atomic sphere and as a Fourier series in the interstitial area using the FP-LAPW approach.

CHAPTER 2

2.1 AIM

The main aim of this work is to study the structural property of compounds $SrTiO_3$ with space group 221_Pm3m under pressure by means of Full Potential - Linearized Augmented Plane Wave (FP-LAPW) method as implemented in WIEN2K code. The motive of the work is to Compare band structure study of $SrTiO_3$ perovskite on bulk and layered phases.

2.2 SCOPE

Important for the understanding of the properties of perovskite compound is a detailed knowledge of structural parameters and with superconducting behavior. The electronic structure and physical properties of the materials can be tuned by layer with various thickness in the compounds.

Some of the recent research of compounds under bulk and surface: For the first time, we have carried out the electronic and optical properties of the orthorhombic bulk and 001-surface of $CsPbBr_3$ from DFT-1/2 approach. The thin flm of CsPbBr3 exhibit tunability of the bandgap via the surface thickness modifcation. The presence of high value of absorption coefficient ∼4.5×105 cm−1 and ∼1.58×105 cm−1 in UV–Vis energy range for both the bulk and the surface, respectively. The tunability of energy bandgap offers remarkable optoelectronic properties in UV–Vis range making this material promising for optoelectronic applications.

2.3 MATERIAL

2.3.1 Perovskites

Perovskites are substances with the chemical formula ABX3. The perovskite family includes all compounds whose structures are generated from an ideal perovskite type with the deletion of certain atoms or with minor lattice aberrations. A cation is monovalent or divalent and may be trivalent in these perovskite compounds, whereas B cation is pentavalent, tetravalent, and trivalent. The structure, physical characteristics, and structures of these perovskite-type compounds have gotten a lot of attention and have been intensively studied in the field. They have long piqued the interest of scientists due to their superconducting, electronic, and ferroelectric capabilities. The remarkable physical properties of perovskite materials, such as their high absorption coefficient, long-range ambipolar charge transfer, low exciton-binding energy, and high dielectric constant superconducting, electronic and ferroelectric properties, and so on, have sparked a lot of interest in optoelectronic and photovoltaic applications.

2.3.2 Bulk material

The intrinsic nanoscale structure of many bulk materials gives them their properties today. Nano-dispersed carbides provide high-strength, low-alloy (HSLA) steels their strength. Precipitates with diameters in the 10–100 nm range are used to reinforce all aerospace alloys based on aluminium, magnesium, and titanium. Due to Cube nanoparticles, the copper alloy wiring connectors found in autos and other electrical equipment continue to be springy and maintain good electrical contact. These are all common alloys with a dispersion that was produced by heat treatment, along with many more. Only a small portion of the volume—typically 1–5 percent—is taken up by the dispersion. The steel, aluminium, and copper matrixes are not themselves nanocrystalline. What if you could make it happen? It's not simple. However, materials scientists enjoy a challenge, and this one hasn't deterred them. Figure 1.2 illustrates the three possible attack directions. The top-down method involves dismantling the structure of a bulk material and shrinking the crystal size to submicron or nanodimensions. The second intermediate strategy begins with typical micron-scale particles and uses milling techniques to downsize their structure to the nanoscale [23].

The third method is to construct the solid from the bottom up, either at the atomic scale or from nanoclusters while maintaining the scale of its structural units.

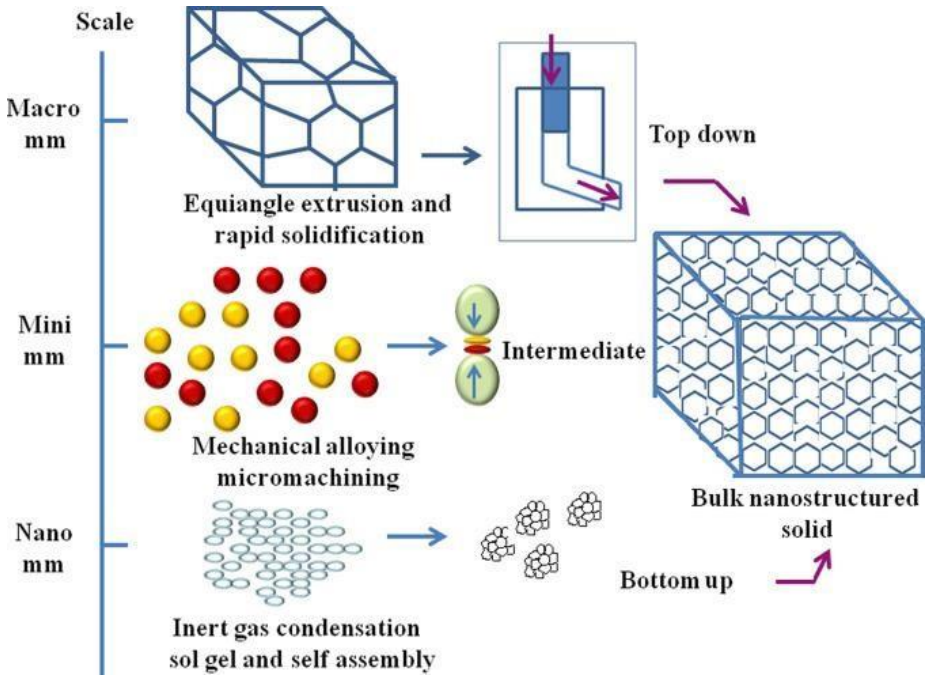

Figure 2.1 Bulk Structure

2.3.2.1 BULK MATERIALS PROPERTIES

Solids in bulk come in a variety of sizes and shapes. These characteristics affect how simple it is to move and store these materials. In contrast to powders, which can compact and block storage or moving equipment, granular materials move more readily because of their uniform shape and big size. Solid bulk qualities include their capacity to flow, which is related to the angle of repose. The material can be stacked as steeply as this angle before it flows downward. Angles up to 90 degrees are possible. Angles that are steeper signify materials that are particularly cohesive and pile up higher before spilling. The following angles show how well the materials flow:

- Very free-flowing: Less than 30 degree
- Free-flowing: 30 to 38 degrees
- Average flowing: 38 to 45 degrees
- Cohesive: 45 to 55 degrees

- Non-flowing: Greater than 55 degrees.

The size of the materials affects the angle of repose. Larger particles have lower angles of repose, allowing for higher flow ability as long as they have a uniform shape. For non-uniform particles, the angle of repose shows a slight increase, which explains the inability of irregular wood chips and similar flaky materials not to flow as well [24].

2.3.3LAYERED MATERIAL

Layered materials are solids having strongly anisotropic internal bonds between two-dimensional sheets, but only weak external bonds between sheets. Layered materials are frequently appropriate for intercalation reactions due to their specific structural characteristics. The structure and chemical makeup of layered materials are discussed, with the exception of those that contain phosphates. Interplanar forces, which are weaker than intraplanar binding forces, hold sheets or planes of atoms in layered materials together. The placement of atomic or molecular guest species between the layers is made possible by this structural design. A controlled change of the physical and chemical characteristics of the host layered material across a broad range is made possible by this insertion (or intercalation), leading to new variants of unique layered materials [25].

There is also a description of the intercalated layered materials. According to the makeup of their layers and the forces holding them together, layered materials can be roughly divided into three classes. The intrinsic resistance of the layers to distortions involving displacements transverse to the layer planes is determined by the interlayer forces.

Type I layered materials are made up of layers of atomically thin sheets. Van der Waals forces keep the neutral layers in place. Graphite and boron nitride are two examples. When it comes to distortions transverse to the layer planes, graphite's layers have a tendency to be "floppy" and are simple to separate. However, against longitudinal in-plane distortions, graphite is stiff.

A few (often three) different planes of firmly bound atoms are kept together by van der Waals forces to form the layers of type II layered materials like dichalcogenides and lamellar oxyhalides.

Layers in materials of type III are composed of dense (up to seven) assemblages of atoms with strong bonds. Layered formations like silicate clays and layer double hydroxides, which are highly stiff to interlayer distortion or expansion, can develop from charged layers, in which case the interlayer force is ionic [26].

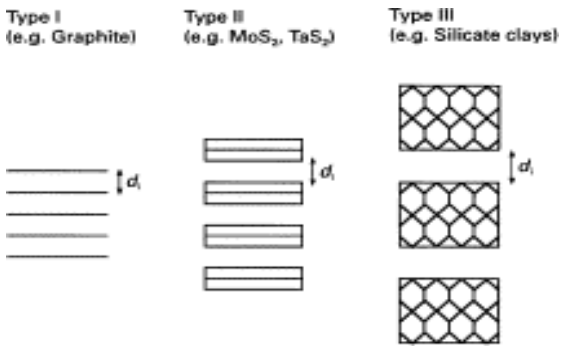

Figure 2.2 Three types of layered materials

2.3.3.1 LAYERED MATERIALS PROPERTIES

The four main themes of the themed issue—Optical, Electronic, Magnetic Properties, and Applications for Energy and Environmental Issues—relate to the characteristics of layered materials. Another topic of the theme issue, which also includes Structural studies of innovative materials, is theoretical research and their advancements in foretelling/modeling structure and properties of layered materials. The issue includes articles of the review kind as well as complete pieces describing original findings (Feature, Highlights and Applications). The relevance of layered materials in presenting new opportunities and strategies for applications in a variety of fields, such as electronics, optics, spin-electronics, energy production and storage, environmental solutions, catalysis and photocatalysis, biomedical applications, and so forth, is

demonstrated in several fascinating reviews in a very effective and elegant manner. This is particularly relevant when dealing with nanostructures or nanosystems, for example, in the field of nanoscience and nanotechnology. It offers a nice and suitable transition from materials with particular qualities to materials that may be altered, constructed, or modified to show a wide range of various properties. The scientists claim that there are still many areas of graphene chemistry that need to be discovered or refined. Starting with the preparation itself, there are yet no synthesis techniques that can produce significant quantities of graphene with a predetermined number of layers. These research appear to be dependent on the possibility of creating the materials by various means; they are also interested in how electronic, magnetic, and electrochemical properties manifest in these materials and the means to control them. Research efforts should also focus on the intriguing impact that graphene has on polymers. These materials also include gas adsorption abilities that could be tuned for use in environmental applications. We present in some detail the synthesis, characterisation and characteristics of single-, bi- and multi-layer graphenes, as well as their potential for molecular charge transfer and electrochemical doping. Organic–inorganic layered materials maydisplay interesting magnetic properties present a novel hybrid cobalt hydroxide pillared by ethanedisulfonate ligands, which exhibits a field-induced magnetic transition [27].

2.3.4 $SrTiO_3$ COMPOUND

$SrTiO_3$ is interesting to study for several reasons. Strontium titanate $SrTiO_3$ is the most significant perovskite in the titanate family (STO). Strontium titanate (SrTi) is a perovskite material with a wide range of O_3 applications, including ferroelectricity, grain-boundary barrier layer capacitors, oxygen-gas sensors, epitaxial growth substrate for high temperature superconductor thin films, and optical switches.

Further interest in $SrTiO_3$ stems from the fact that it is widely used as a substrate for thin-film growth of perovskite structures or structures containing perovskite-type

structural blocks like high-temperature superconductors. It is well known that the deposition of thin films can lead to large strain effects at the film–substrate interface. Due to the ability of these materials to separate photo-generated carriers (electron and hole), perovskite oxide-based semiconductors such as $SrTiO_3$ (STO) play an important role in photovoltaic and photocatalytic applications. Many researchers have recently become interested in titanates since some titanates are employed as ferroelectric, electroconductive, photorefractive, and photovoltaic materials.

Energy demand is increasing in tandem with increased energy and environmental concerns. As a renewable green energy, the use and transformation of solar energy has become a prominent study topic.

For many years, scientists have been developing solutions to help humanity tackle the looming threat of climate change. They are all looking for sustainable energy sources to replace the harmful fossil fuels. Strontium titanate ($SrTiO_3$), a crystalline substance that can be used as a "**photocatalyst**" in **solar devices**, can point us in the right way.

CHAPTPER 3

3. COMPUTATIONAL DETAILS

3.1 WIEN2k

WIEN2K CODE

WIEN2k is one of the most efficient and dependable simulation codes available. This programme was used to execute all of the computational work provided on lanthanide intermetallic compounds [28]. WIEN2kis a full-potential all-electron code developed at the Institute for Material Chemie, Technical University of Wien, Austria, by Blaha et al. WIEN2k is made up of numerous independent F90 programmes that are linked together using C-shell scripts. The code is based on the DFT Kohn-sham formalism.[29] The code initially starts from structure generating document comprising information on space group, lattice parameters, atomic species, atomic location, muffin tin radii, etc. The materials are initialised in a step-by-step process based entirely on the input values: I NN distance- determine the atomic sphere radius by checking for overlapping spheres, coordination numbers, and nearest neighbour distances. (ii) SGROUP- computes the point and space groups for the specified structure. (iii) SYMMETRY- calculates the point group of the particular atomic sites and checks the symmetry operations. LSTART- computes atomic densities for all atoms. (iv) KGEN- creates a Brillouin zone k-mesh. (v) DSTART generates a starting density for the SCF cycle using atomic density superposition.

The self-consistent strategy is an iterative approach that includes selecting the Schrödinger equation to obtain a more precise set of orbitals, then solving the Schrödinger equation with theses until the results converge. The scf cycle begins with LAPWO, where the total potential is calculated as the sum of the coulomb and exchange correlation potentials. LAPW1 then obtains the Eigen values and Eigen vectors of the valence states by diagonalizing the Kohn-Sham equation and setting the Hamiltonian and the overlap matrix. LAPW2 then computes Fermi energy and generates valence charge density.

In the LCORE, the states and energies of the core electron are calculated one at a time in an ordinary atomic calculation, yielding the overall core density. Overall density is the sum of core and valence density. Because the density frequently differs greatly from the old density, MIXER mixes them to avoid large swings between iterations that could lead to divergence. WIEN2K checks for the new and new density at the end of the cycle; if they differ, a new iteration with new density is initiated. This method is continued until the original and new densities match.

In order to solve these equations, we have to construct the effective Hamiltonian operator which depends on the electron density of the electronic system. The manner through which the Schrodinger wave equation solved within Code WIEN2kis represented by the flow chart.

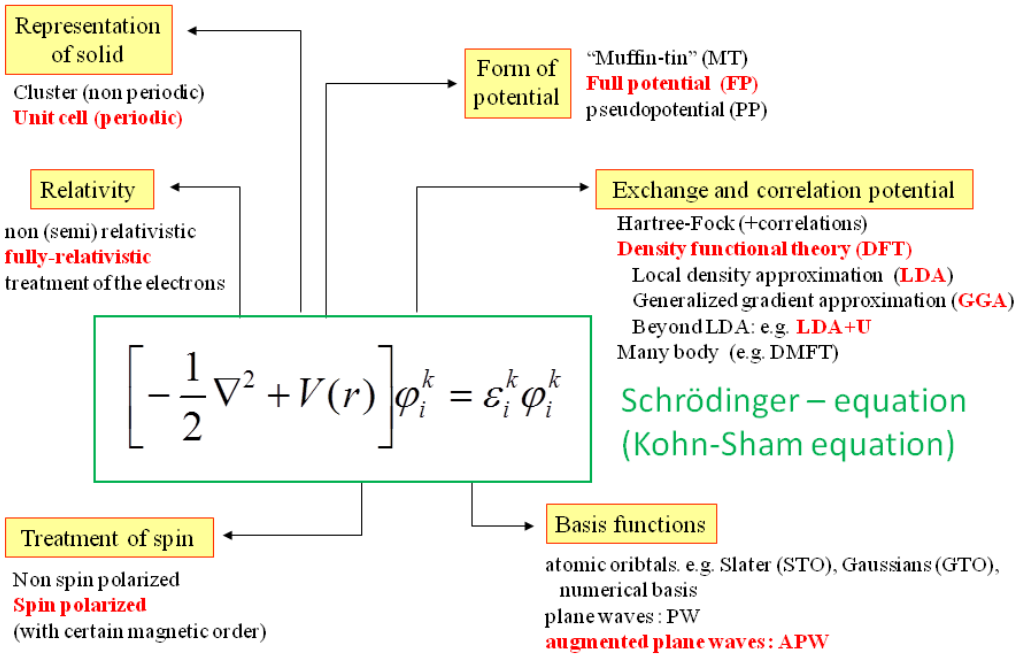

Fig.3.1. FLOW CHART OF WIEN2K

3.2 PROPERTIES OF WIEN2K CODE

The following are the considerations made in the development of the new Wien2k package that are required for modern computer code.

a) Accuracy

To do this, a well-balanced basis set is used, which contains numerical radial functions that are calculated in each iteration cycle. As a result, these functions are accurate near the nucleus and respond to charge transfer or hybridization processes. It's a full-potential, all-electronic approach. Solving Dirac's equation is analogous to dealing with relativistic issues (including spin orbit coupling). Atoms from the periodic table can all be handled.

b) Efficiency and Performance

This requirement is best met by the new mixed base APW+lo/LAPW. Smaller matrix sizes save computer time, allowing larger systems to be studied.

c) Parallelization

If the memory requirement exceeds the capacity of a single CPU, the programme can be performed in parallel, either in a coarse grain scheme in which each k-point is computed on a single processor or in a fine grain scheme in which each k-point is computed on several processors.

d) Architecture

Based on the architecture, efficient algorithms and libraries are used during the installation of the application package.

e) Portability

It necessitates the use of industry standards such as FORTRAN90, MPI, BLAS, SCALAPACK, and so on whenever practical.

f) User friendliness

It is achieved by a web based graphical user interface (GUI), called w2web. The program package provides an automatic choice of default options and it is also complemented by an extensive User's Guide.

3.3 APPLICATIONS OF WIEN2K

So far, insulators, semiconductors, (transition) metals up to f -electron systems, and intermetallic compounds have been explored in QM calculations using the LAPW technique (used in various versions of the Wien code). A quick description of several applications is provided below.

i) Band structure and density of states (DOS) calculations

The energy band structure and matching density of states are critical elements in determining the electronic structure of a system. Their investigation offers details on the electric properties (metal, insulator, or semiconductor) as well as chemical bonding.

Site decomposed partial densities of states can be used to calculate the strength of interactions between the orbitals of the constituent atoms. The band structure is very important in the context of photoelectron spectra.

ii) Electron densities

The electron density is the most essential quantity in DFT. Using the Fourier transform, the static structural factors may be easily estimated and compared to experimental X-ray diffraction data.

iii) Electric field gradients (EFG)

Because the EFG is uniquely defined by charge distribution and thus electron density, it can be determined from fundamental principles. The nuclear quadrupole interaction (NQI) determines the anisotropy of the charge density distribution near the nucleus, which can be investigated using nuclear magnetic resonance (NMR), nuclear quadrupole resonance (NQR), Mossbauer, or perturbed angular correlation (PAC) experiments.

iv) Total energy and phase transitions

With total energy in hand, the relative stability of different phases can be determined by holding as many parameters constant as possible to compensate for systematic errors.

v) Forces and structural optimization

Understanding the forces acting on atoms when they occupy generic positions that are not specified by crystal symmetry aids in the optimization of structural parameters. Forces may be estimated in Wien2k and are essential for such optimizations.

vi) Spectra

Photoelectron spectra, X-ray emission spectra, and absorption spectra can be approximated using partial densities of states and transition probabilities between valence and core states. Such spectra reveal the local binding condition of the atom whose core state is involved. Using the Kramers- Kroening relation, electronic response can be used to calculate optical spectra and related quantities such as the

energy dependence of the real and imaginary parts of the dielectric constant, which can then be used to calculate absorption coefficient, refractive index, electron energy loss spectrum, and reflectivity.

vii) Others:

WIEN2k has been used to investigate several aspects for a wide range of structures, including chemical bonding, structural stability, high-pressure phases, Jahn–Teller distortions, charge distribution, phase transitions, ferroelectric, ferroelectric, or elastic properties. The functions of spin and orbital magnetic moments, magnetic ordering (ferro-, ferri-, antiferro-magnetic), and meta-magnetism in magnetic materials were investigated (including intermetallic compounds). LAPW simulations have benefited optical, core-level, photoelectron, Mossbauer, and NMR spectra.
The magneto-optical Kerr effect, as well as electric field gradients, are all covered. Flaws, such as impurities, can be represented by analysing a super-cell 2x2x2 (or greater), i.e. doubling the original unit cell in all three dimensions. When one of the atoms in this massive unit cell is replaced with an impurity atom, the adjacent atoms can relax into different equilibrium states.

A regular repetition of such a super-cell can approximate an isolated contaminant. Super-cells can also be used to imitate surfaces and their interactions with atoms or molecules. Whether or not they are genuine, hypothetical or artificial structures can be analysed and their properties computed. These computations can be used to anticipate a system's attribute (e.g., insulator or metal) or to determine its magnetic structure.

It is possible to simulate system changes caused by deformations, pressure, or substitutions. The density of states (DOS), partial density of states (PDOS), electronic band structure, and frequency dependence of linear optical properties such as the real and imaginary parts of the dielectric constant, refractive index, reflectivity, and electron energy loss spectra (EELS) of PbMoO4, BaWO4, and NaBi (WO4)2 were calculated using the WIEN2k programme.

CHAPTER 4

4. RESULT AND DISCUSSION

4.1 STRUCTURAL PROPERTIES

The structural optimization is the initial stage in DFT computations. The original structure can be deduced from experimental data in the vast majority of cases. For good results, the DFT energy E_{TOT} can be estimated. Understanding the forces acting on atoms at general positions that are not controlled by crystal symmetry aids in the optimization of structural parameters. WIEN2k has the ability to calculate forces, which are crucial in such optimizations. As a function of cell volume energy, the atoms' muffin tin radius (RMT) is also tuned.

The crystal structure of $SrTiO_3$ is cubic and space group is Pm-3m_221. The basis set corresponding to RKmax was used for all calculations. The convergence parameter RMT* Kmax which controls the size of the baris set is set to 7. Where Kmax is the highest value of the reciprocal lattice vectors and RMT is the muffin tin sphere's (MT) smallest value. The calculations are repeated 1000-k times to ensure self-consistency. The resulting structure is then saved. With k-points equal to 1000, RMT*Kmax equal 7, and scf (self-consistent field) cycle runs, the initialization computations are performed. The scf cycle is run for different k-points between 1000 and 5000. The K-points with the least energy are chosen. The K-point with the lowest energy for $SrTiO_3$ is 1000. Volume optimization is carried out and the graph is plotted between volume[a.u.^3] and energy [Ry]. Figure 4.3 represents the volume optimization graph. The total energy of the given system is obtained and then fitted into the Birch-Murnaghan equation of state.

- Convergence parameters:

  Energy - below 0.0001Ry

  Charge - below 0.001Ev

  K-Points-1000 $(10 \times 10 \times 10)$

VOLUME OPTIMIZATION AND BOLK MODULUS

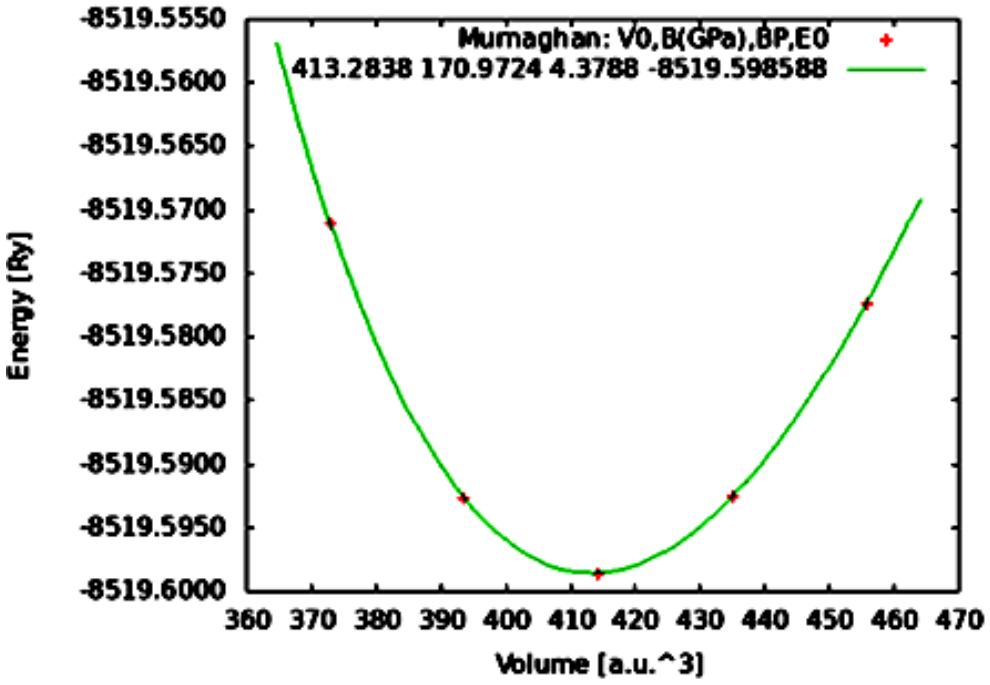

Figure 4.1 volume optimization

Volume	Energy
372.8899	-8519.571041
393.6061	-8519.592643
455.7544	-8519.577334
414.3222	-8519.598579
435.0383	-8519.598579

Table 4.1 Volume vs Energy

Volume optimization is carried out and the graph is plotted between the volume and energy. Using Birch-Murnaghan Equation of state studies. Optimized lattice parameter, Volume and its energy are listed in Table 4.1 The Birch-Murnaghan equation of state is used to determine the optimum lattice parameter for $SrTiO_3$ from the optimized graph. The resulting lattice parameter values are provided in the construction of the $SrTiO_3$

structure, and the initialization calculation is finished along with the scf cycle. As a result, $SrTiO_3$ is formed in bulk. Fig 4.2 gives the bulk $SrTiO_3$.

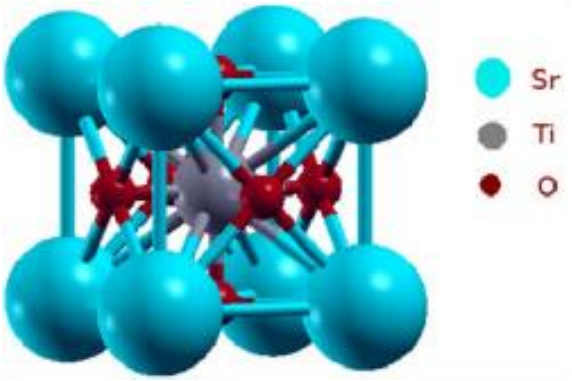

Figure 4.2 (i) Reference of Bulk $SrTiO_3$ crystal structure

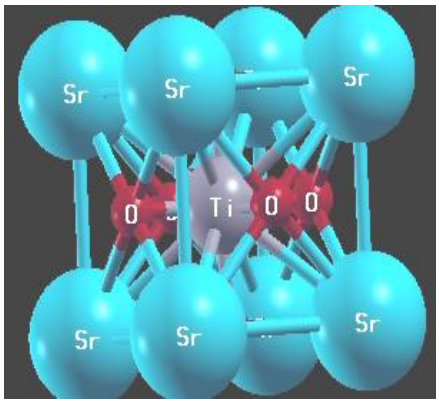

Figure 4.2(ii) $SrTiO_3$ crystal structure of this present study

Fig 4.3 CRYSTAL STRUCTURE OF LAYERED PHASE OF DIFFERENT THICKNESS OF CUBIC $SrTiO_3$

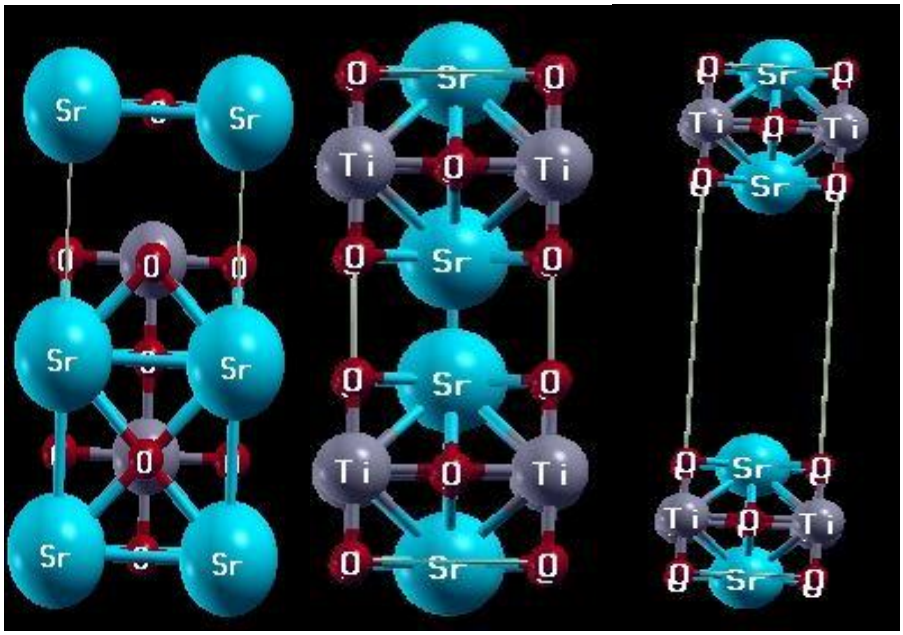

Layer at top surface | Two layer separated by distance 5a.u. | Two layer separated by 18.897au

Table 4.2 Structural and electronic parameters of $SrTiO_3$

Parameter	**STO**	**Bulk separated by a single layer**	**Bulk separated by two layer at distance 5au**	**Bulk separated by two layer at distance 18au**
Optimised "a"(lattice constant in a.u.)	a=b=c=7.744 (a=7.445) [16]	a=b=7.448 (a=7.388) [21] c=16.8974	a=b=7.448 c=19.8969	a=b=7.448 c=33.7943
Volume (V) a. u^3	413.2772	503.4073	313.6799	532.7762
Space group	221_Pm-3m	99(P4 mm)	123(P4/mmm)	123(P4/mmm)
Lattice type	Cubic Primitive	Tetragonal Primitive	Tetragonal Primitive	Tetragonal Primitive
Band gap(eV)	1.966 eV 1.92 eV[ref12]	1.853eV	2.258eV	1.791eV
Fermi Energy (Ryd)	0.4561	0.3739	0.4314	0.1598
Total Energy (Ryd)	-8519.5986	-17039.0918	-23549.4183	-23549.5748
Bond length in a. u	5.2671 (Sr-O) 6.4508 (Sr-Ti) 3.7244 (Ti- O)	5.2671 (Sr-O) 6.4508 (Sr-Ti) 3.7244 (Ti- O)	5.2671 (Sr-O) 6.4508 (Sr-Ti) 3.7244 (Ti- O)	5.2671 (Sr-O) 6.4508 (Sr-Ti) 3.7244 (Ti- O)
Bond angle in deg	54.736 (Sr-Ti-O)	54.74 (Sr-Ti-O)	54.74 (Sr-Ti-O)	54.74 (Sr-Ti-O)
Electronic specific heat coefficient(C_V) J/(kg K)	3.93	0.05	5.06	0.14
Debye temperature(k)	628.654	465.513	517.448	392.749
DOS ($N(E_F)$ Ryd	22.67	0.30	29.21	0.81

External pressure is supplied to the compound for various V/Vo values, and the corresponding pressure experienced by the compound is calculated using the volume derivative of the Birch-Murnaghan EOS. As shown in the table 4.1, the DOS and FE does increase and decrease respectively due the thickness increase and there is decrease in the band gap that result in the compound being an superconductor for all the applied thickness. we can observe DOS value also increases from 22.67 to 29.21 as expected, the FE decreases from 0.4561eV to 0.1598eV as the distance increases.

4.2 ELECTRONIC PROPERTIES

Electronic band structure provides crucial information about the conceivable energy ranges that electron can inhabit (that is, energy bands) as well as the energy areas that cannot be occupied (named as band gap). In insulators and semiconductors, the electronic band gap is calculated by subtracting the valence band maximum (VBM) from the conduction band minimum (CBM). Calculations of electronic band structure describe the probable electronic transitions from VBM to CBM.

Density of states and electronic band structure often provide sufficient information for a through characterization of the electronic properties of a material. The energy band structure, total density of states (DOS) of $SrTiO_3$ were calculated by FPLAPW and methods. For the optimum parameters, the compound's band structure and DOS are determined. Figs. 4.4 show the theoretical band structure for the $SrTiO_3$ as well as the density of states that go along with it. Our calculations show that the valence band maximum and the conduction band minimum are located at Γ having direct bandgap with different bandgap energies for different layer structures.

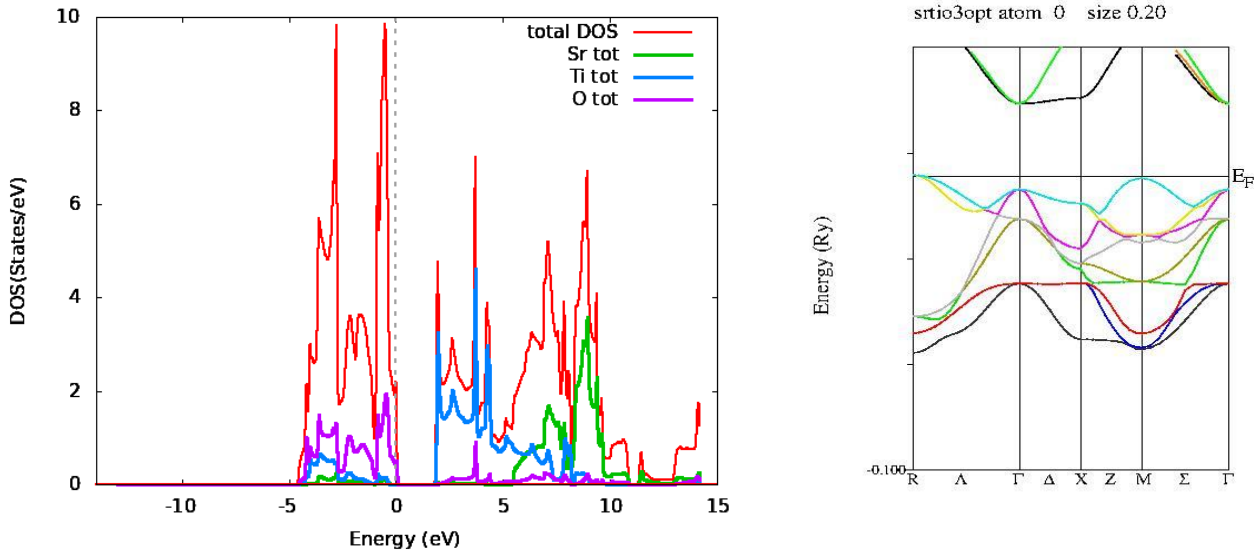

Fig 4.4 (a) The band structure and the DOS of bulk cubic $SrTiO_3$.

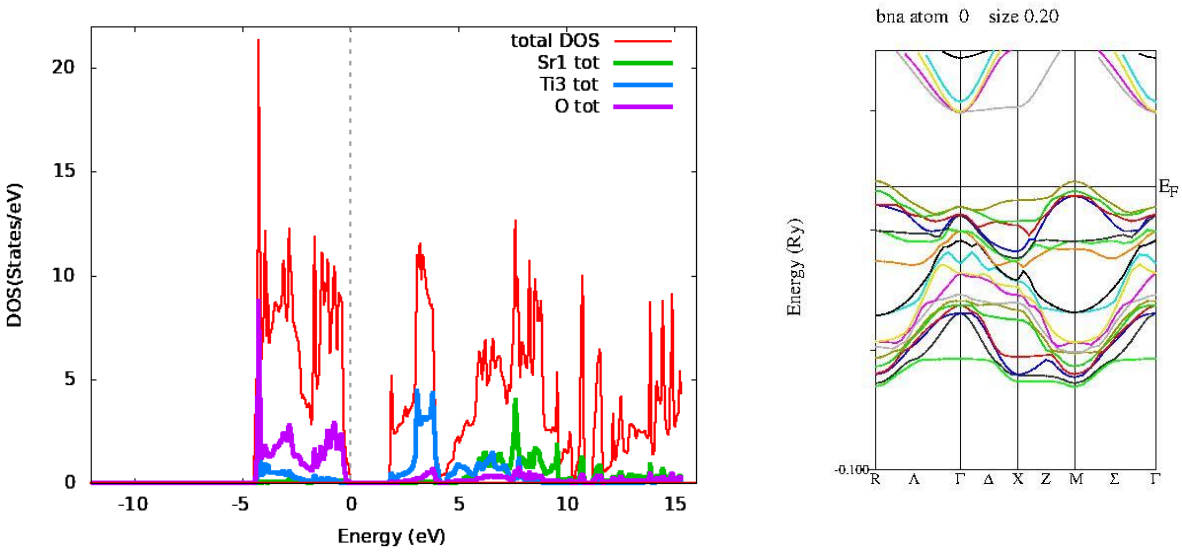

Fig 4.4(b) The band structure and the total DOS of Bulk separated by a single layer.

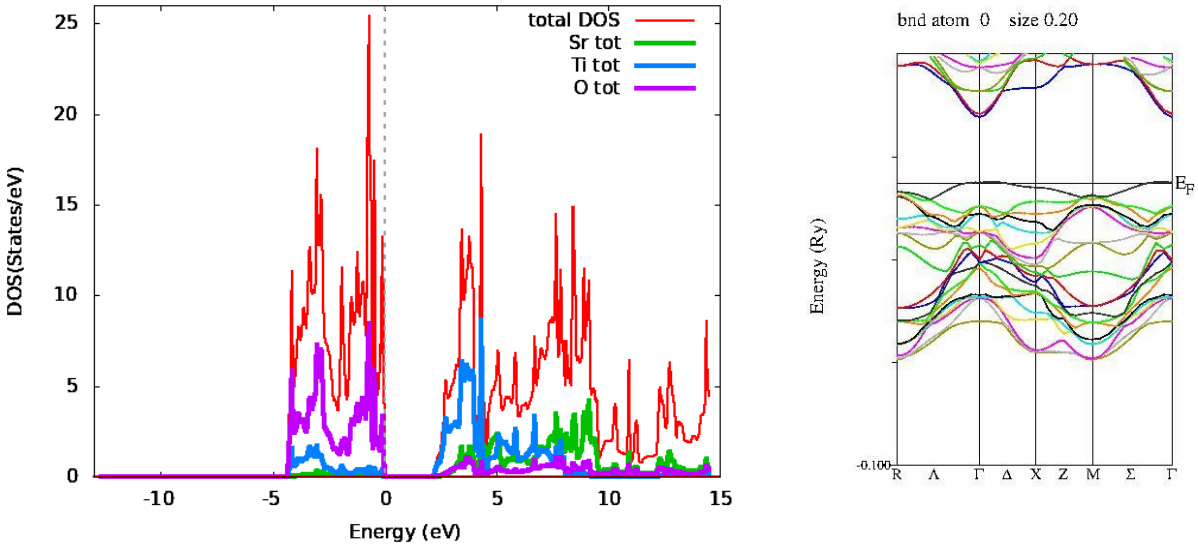

Fig 4.4 (c) Bulk separated by two layers at distance 5a.u.

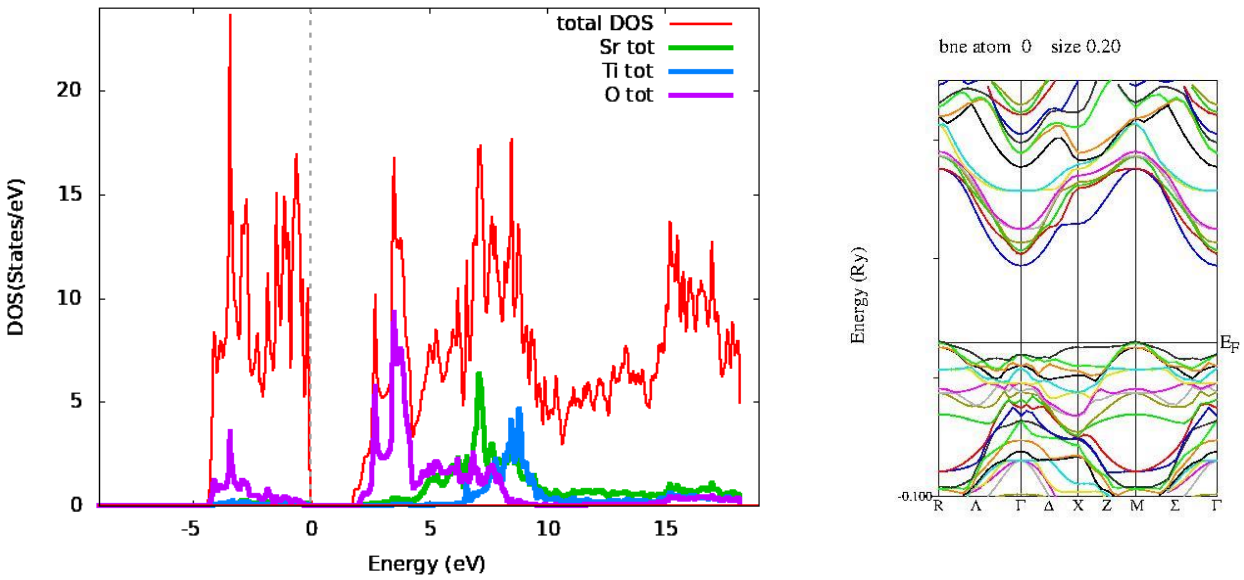

Fig 4.4(d) Bulk separated by two layers at distance 18a.u.

4.2.1Density of state

The density of states (DOS) is essentially the number of different states at a particular energy level that electrons are allowed to occupy, the number of electron states per unit volume per unit energy. As we can see in the figure 4.4 the graphs indicate the density of state (DOS) increases this is due to the increase in the thickness. Figure 4.4 represents the density of states (DOS) histogram. The DOS is plotted in terms of Ryd (Rydberg). The x and y axis are adjusted to get a clear view of the histogram. The histogram is plotted between Energy (Ryd) and DOS (states/Ryd). The density of states is an important parameter for the calculation of the electronic, optical, chemical and magnetic properties of material. These graphs show bandgaps. The energy bandgaps shows that they are semiconductors. The valence band for $SrTiO_3$ in figures 4.4 a, b, c, and d is generated by the O-p state, with minor contributions from the Ti-d, Ti-p, and Sr-d states. The bands in the conduction band are caused by the Ti-d and Sr-d states, with a minor contribution from the O-P states. O-p states make up the majority of the valence band, while Ti-d and Sr-d states make up the majority of the conduction band. In Fig 4.4 a, b & c, above the fermi level Ti orbitals influence the electronic structure Sr & O atoms. Titanium is a very excellent material used for solar cells since it has more photovoltaic properties. Thus, these $SrTiO_3$ materials will be more efficient materials for optical devices which has similar results with literature [15].

4.2.2 Band Gap

The band gap (E_G) is the gap in energy between the bound state and the free state, between the valence band and conduction band.

Therefore, the band gap is the minimum change in energy required to excite the electron so that it can participate in conduction.

As shown in the figure 4.4, the fermi level is set at zero eV, $SrTiO_3$ is a direct semiconductor the band gap decreases as the distance increases.

- Fig(i) It is clearly seen that the conduction band (CB) minima and maxima of the valence band (VB) lies at the same value of momentum at Γ symmetry point. By considering these two symmetry points the computed bandgap (Γ - direct band gap) is 1.966eV, and comparable values of band gap of are also reported in the literature [12] are good in agreement.
- Fig (ii) & (iii) The direct band gap (Γ) energies of $SrTiO_3$ determined from the band structure calculations are 1.853eV and 2.258eV are in agreement with direct bandgap 1.89eV and 2.22 eV, respectively, from literature (10).
- Fig(iv) The calculated direct bandgap (Γ) is of 1.791eV close to the direct bandgap value of 1.792eV seen here and in the literature (13).
- These are even consistent with compared the experimental value of the band gap is 1.92 eV [18] and 1.9 eV [19]. This is well known for calculations in the LDA.[14] These results are in good agreement with theoretical LDA results from Cappelini et al. [14] who calculated values of 1.90 and 2.24 eV for the direct band gap, respectively.
- These bandgaps show that these are good semiconducting materials. Thus when distance increase between the two layered structure the bandgap decreases gradually and the material with small bandgap energies values the more efficiency of optoelectronic materials based on $SrTiO_3$.

4.3 OPTICAL PROPERTIES

We explore the effect of layer in the $SrTiO_3$ lattice since $SrTiO_3$ is an active component of optoelectronic devices. The interaction of light with matter is described by optical qualities including the energyloss, refractive index, dielectric function, optical conductivity, and reflectivity, describe the interaction of light with matter.

Utilizing the WIEN 2K code, the dielectric function of the suggested compound [ε (ω) = ε1 (ω) + iε2 (ω)] is calculated from the optical characteristics. Real ε1 and imaginary ε2 are the two components of the dielectric function.The absorptive portion of the optical property is represented by the hypothetical dielectric function (iε2 (ω)). Each spectrum is broken down into pairs of contributions, and the origin of various peaks is then examined using this information. This explains the contributions from the Brillouin zone at various K-points and enables the identification of optical spectrum characteristics with microscopic origin. The transfer of electrons from the valence band into the bottom three conduction bands is the primary source of the optical spectra's contribution.

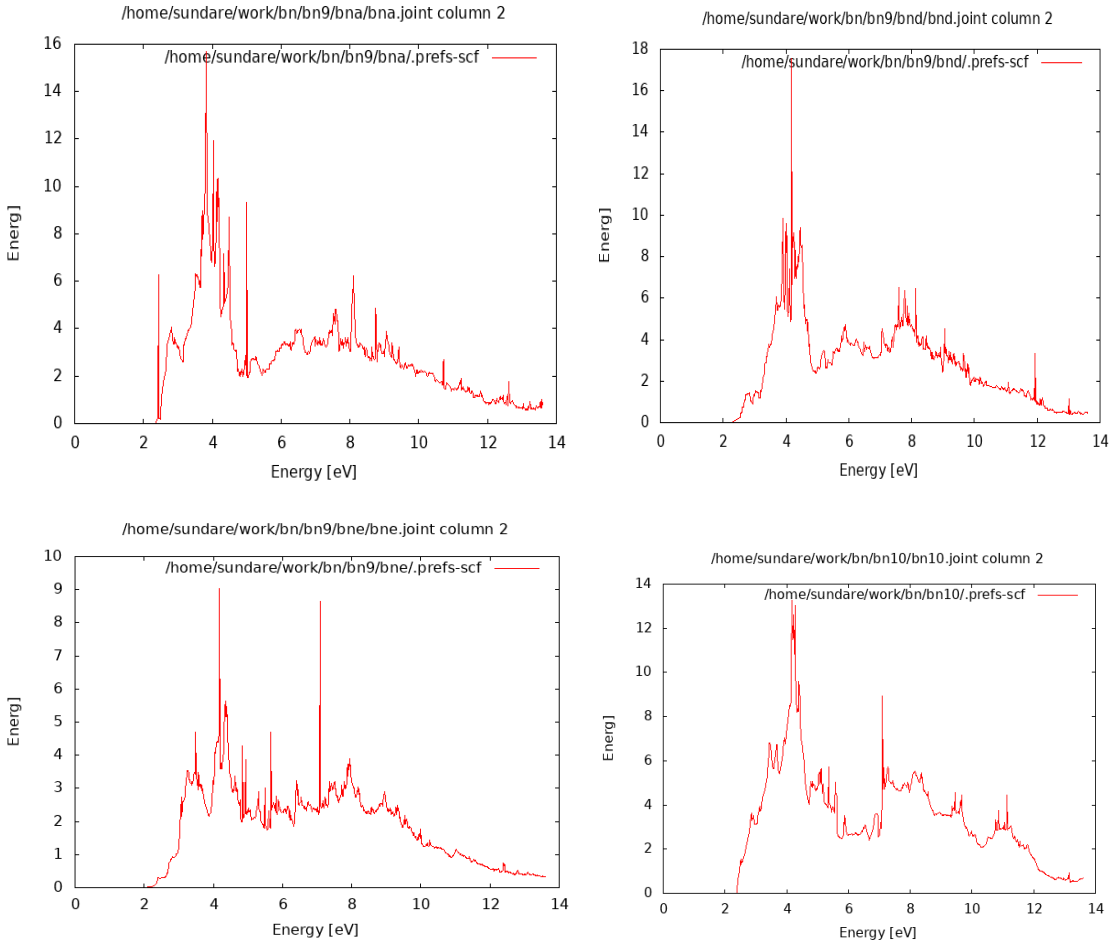

Figure 4.5.(a) The dielectric function(imaginary)

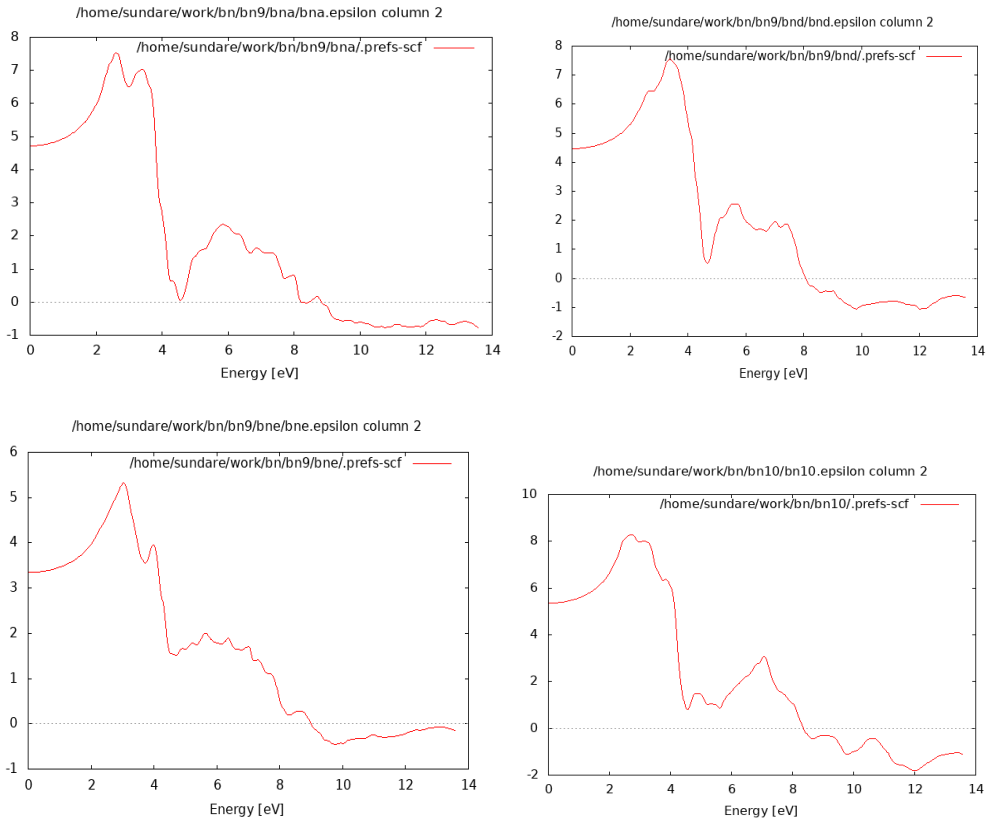

Figure 4.5(b) The dielectric function(real)

In Figure 4.5(a)&(b) gives the imaginary and real parts of dielectric function are illustrated for $SrTiO_3$, respectively as a function of photon energy in the range from 0 to 14 eV. It can be seen from the that is starting to have a considerable value from 2.2 eV for $SrTiO_3$.After threshold energy, we observed some peaks; these peaks originate from electrons transitions from valence band to conduction band. Threshold energies of $SrTiO_3$ are 2.4 eV. The exponential rise after reaching the first peak at 2.8eV is caused by the strong valence to conduction band transition with respect to energy gap. Evaluating the peaks of the dielectric function, ε2 and the corresponding Energy from the Fig 4.3.1 will explain the nature of transitions related to the optical spectra.

From the graph it can be seen all compounds are optically similar.

The real part (ε gives us information about the polarizability of a material. From the figure the inactive dielectric constant ε1(0) can be evaluated and it is a very important quantity determining a materials semiconducting property. The value of ε1(ω) at zero energy is the static dielectric constant ε1(0). ε1(ω) has values between 7.6, 6.4 and 5.5eV. The negative values of real dielectric constant which is in the ultraviolet spectrum for $SrTiO_3$; show a metallic behavior of these compounds in the mentioned regions.

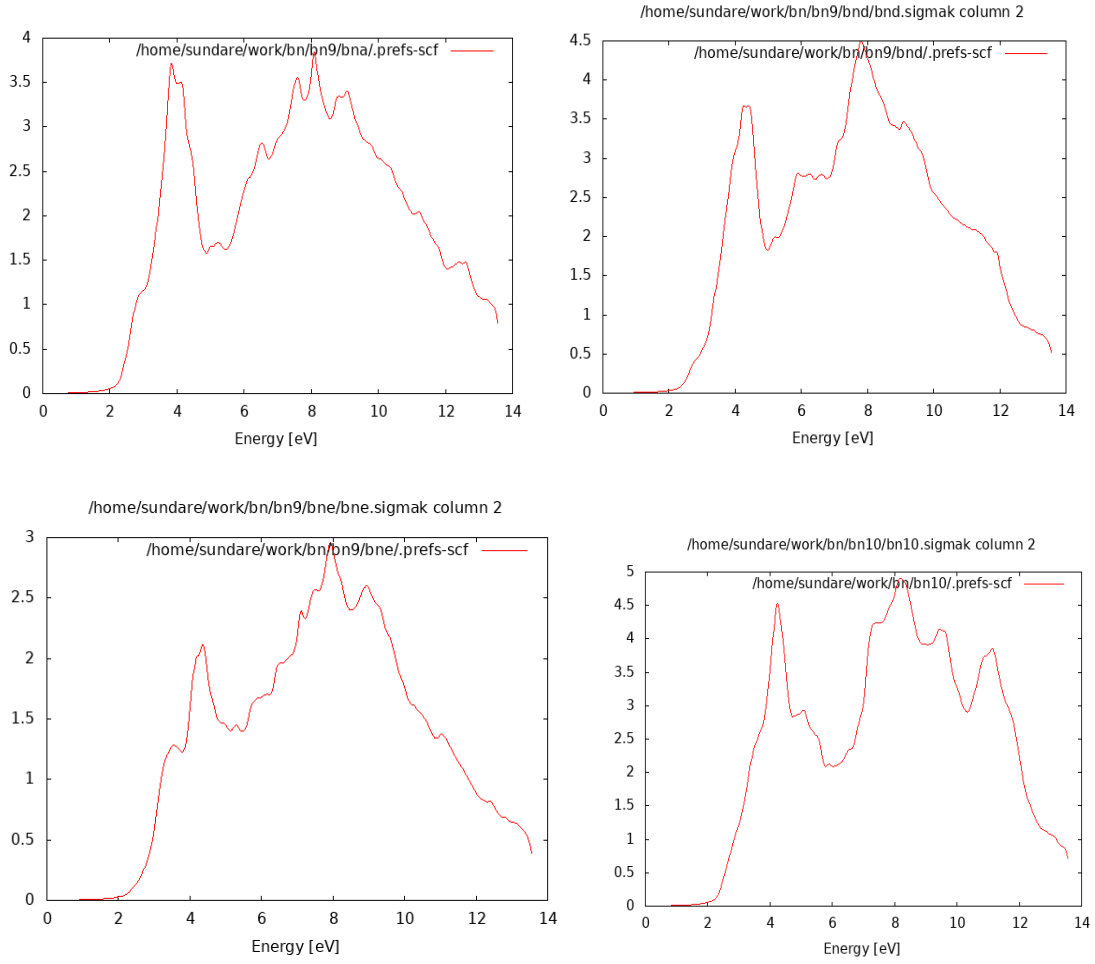

Figure 4.5(c) Optical conductivity

Optical Conductivity σ(ω) describes the conduction of free charges over a particular range of Photon energy. Fig 4.5(c) represents the optical conductivity of $SrTiO_3$, σ in terms of the energy. The main peak of σ(ω) is at 3.8, 4.2 and 4.4eV respectively. There are many major peaks for Fig 4.3.3, these points exhibit excitonic feature. Excitons are bound electron-hole pair and they move around the crystal transporting energy, the sudden peak in the optical conductivity is caused by the excitons. The main peak of the function σ(ω) for the compounds from the figure corresponds to the maximum optical conductivity σmax (ω). The value of σmax (ω) for $SrTiO_3$ is 3.7, 4.5 & 3. We have also observed some peaks in the conductivity spectra of the studied compounds. The conductivity increases as the material becomes more photons (energy) absorbent.

The energy loss function L(ω) is describing the energy loss of the fast electrons propagates inside the material. The energy loss spectra of $SrTiO_3$ are depicted in Figure 4.5(d). We observe some peaks, the highest peaks related to the plasma frequency [20]. From figures the plasma frequency of $SrTiO_3$ occur at 13eV whereas the experimental peak appears at about 29 eV. It is clear that the energy loss function gets its minimum value corresponding to the higher value of the imaginary part of dielectric function, which is the main characteristic of semiconductors [15].

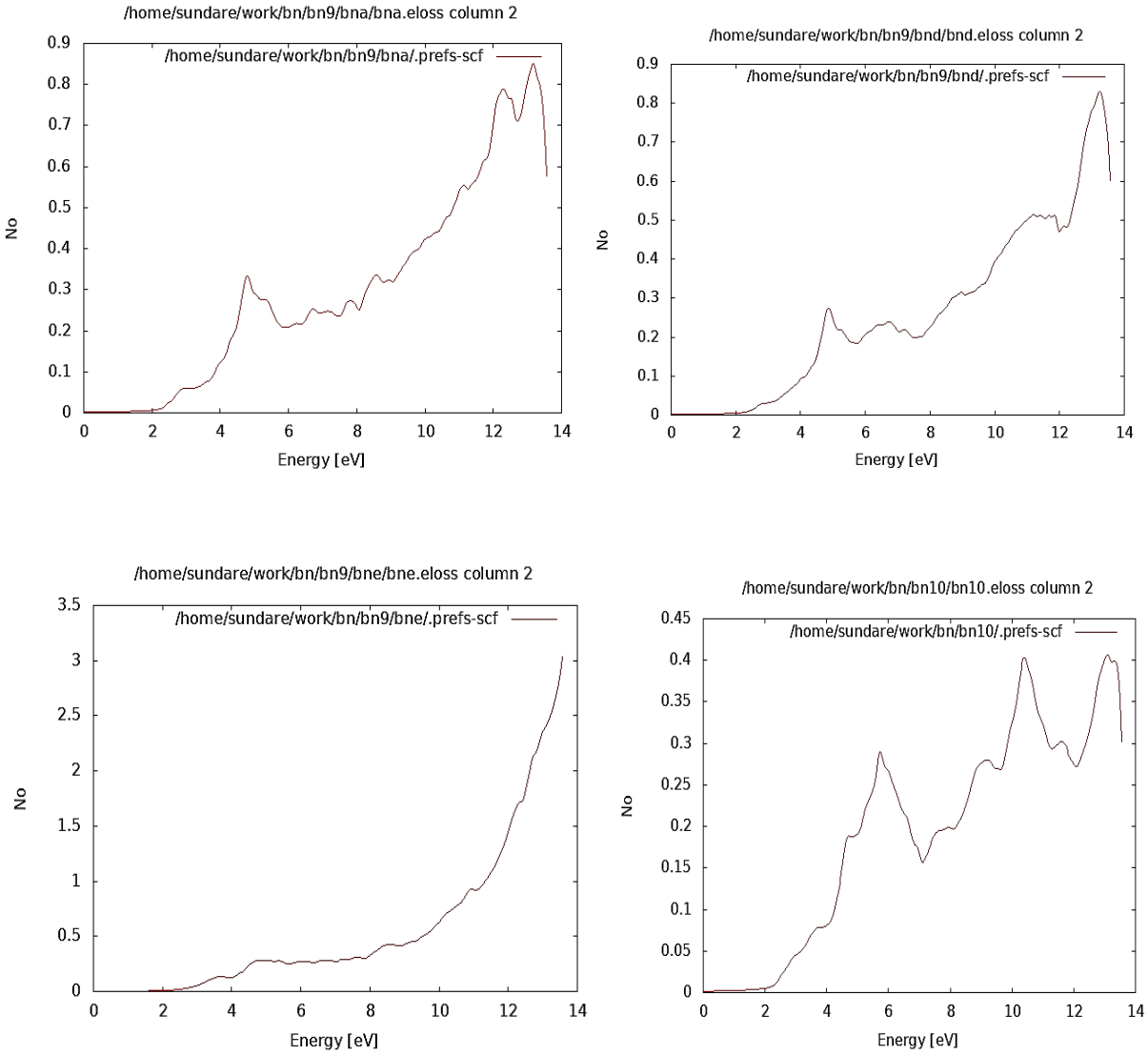

Figure 4.5(d) Energy loss spectrum

Fig4.5 (e) Reflectivity graph

Fig 4.5(f) Refractive index graph

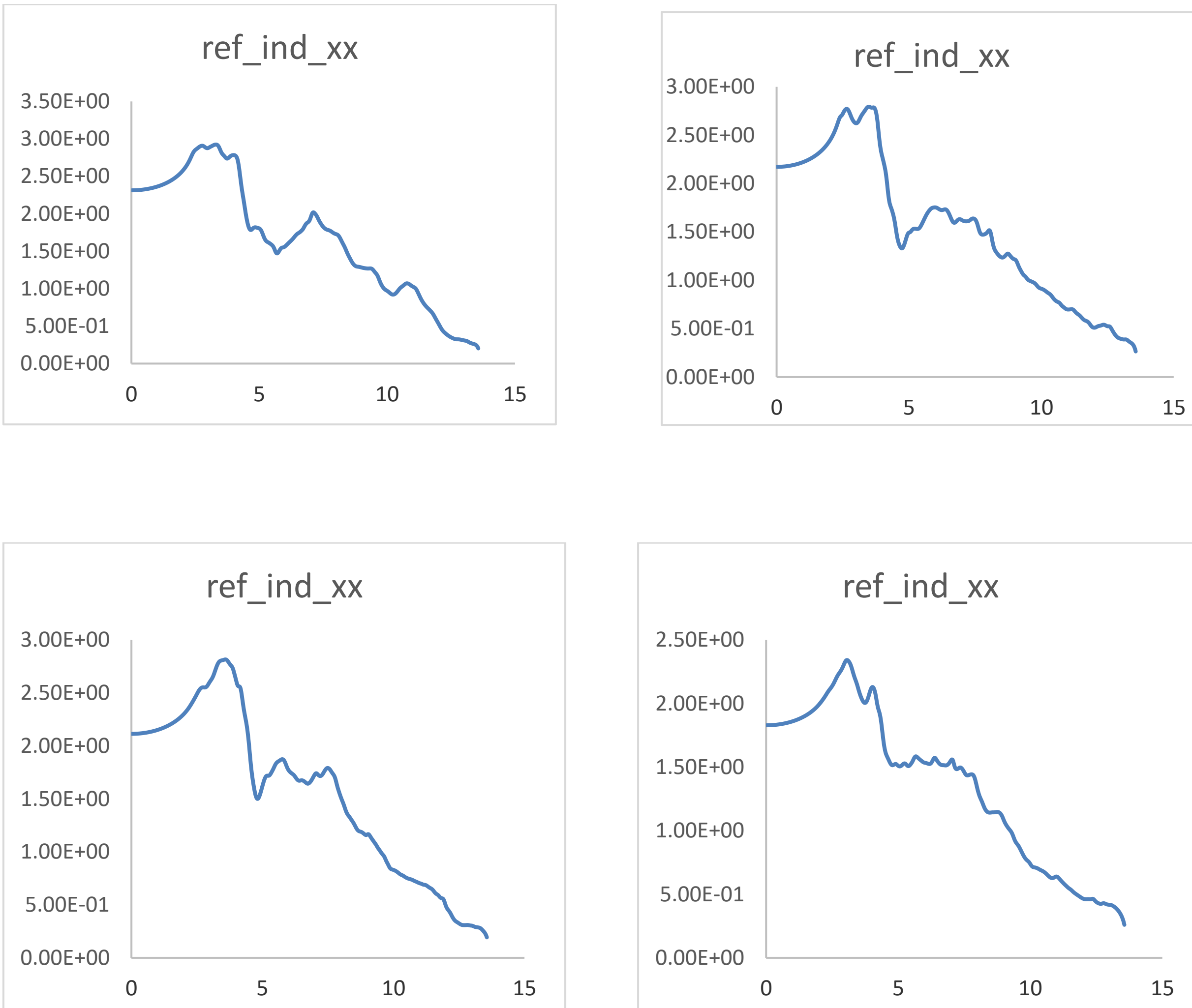

Table 4.3 Reflectivity and refractive index vs Energy

Crystal structure	Reflectivity @ Energy	Refractive index@Energy
Bulk	0.336733@4.4490	3.36061@2.91885
Bulk separated by a single layer	0.313417@4.01368	3.3334@2.75419
Bulk separated by two layers at distance 5a.u.	0.312433@4.5307	3.5783@2.81575
Bulk separated by two layers at distance 18.897a.u.	0.190906@4.47627	3.14292@2.32756

The reflectivity's spectra of $SrTiO_3$ as a function of energy are shown in Figure4.3.5. The static reflectivity of $SrTiO_3$ is 0.15. The reflectivity value increased rapidly in the high energy region; far ultraviolet region (FUV); for all bulk and layered $SrTiO_3$ compounds, all compounds are suitable as wave reflectance compounds in the (FUV) region, but unsuitable as transparent compounds. Similarly, the reflection is observed to be maximum at all points where the absorption is minimum.

The calculated refractive index (n) for these bulk and layered structure are 3.36, 3.33, 3.57 & 3.14 which are slightly greater than n=2.95 of literature [15]. The calculated values are good in agreement with other theoretical works. Maximum value of refractive index at zero photon energy is associated with the lowest absorption energy. As the absorption increases, the refractive index goes on decreasing as shown in figure 4.5(e).

4.4 THERMAL PROPERTIES

Fig 4.6 (i)Gibbs free energy, (ii)Bulk modulus and (iii)entropy vs T relation for bulk separated by single layer

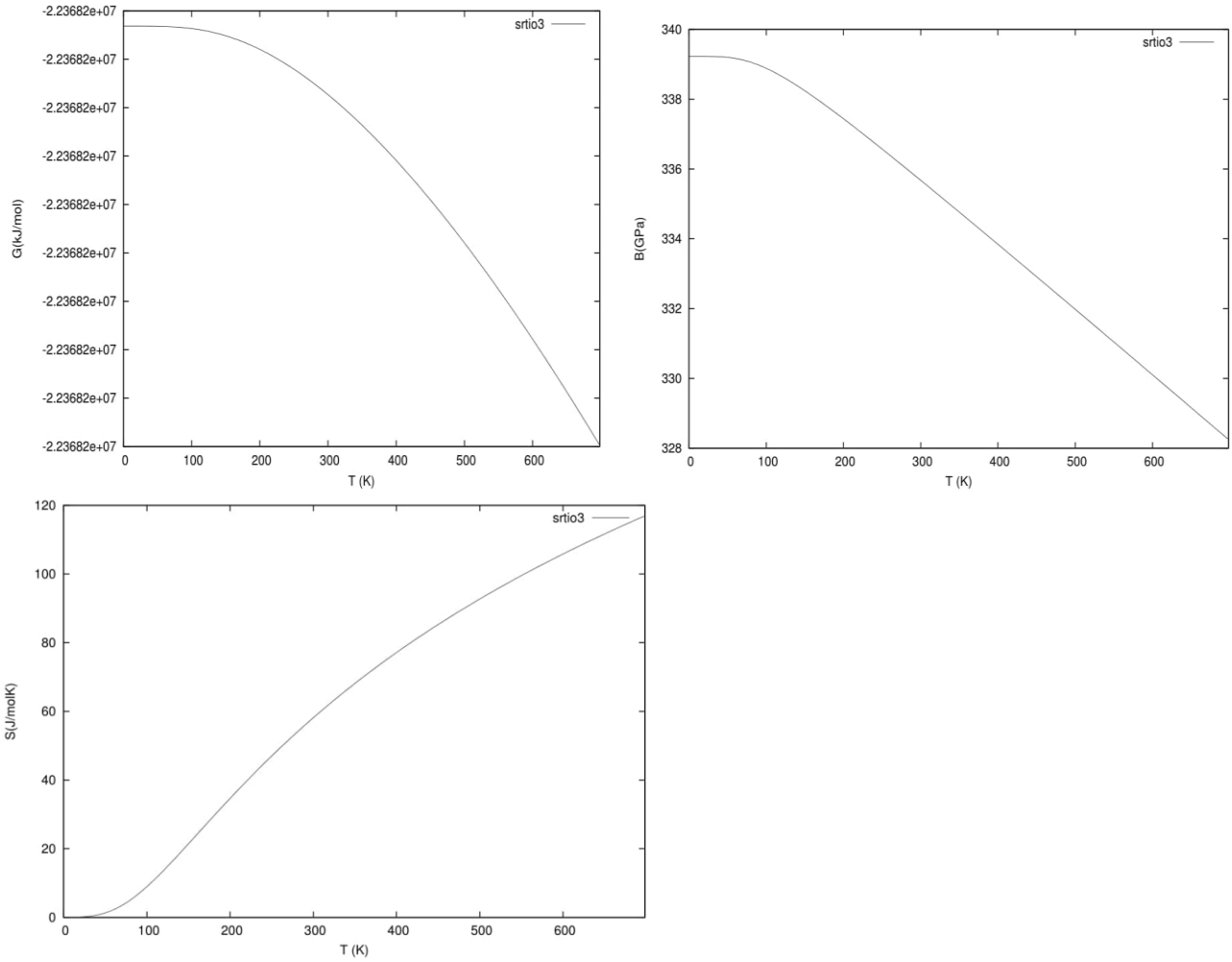

Fig 4.7 (i)Gibbs free energy, (ii)Bulk modulus and (iii)entropy vs T relation for bulk separated by layer at distance 5a.u

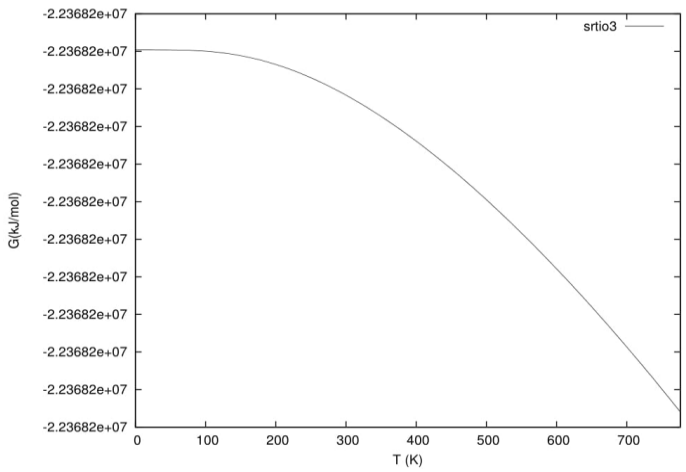

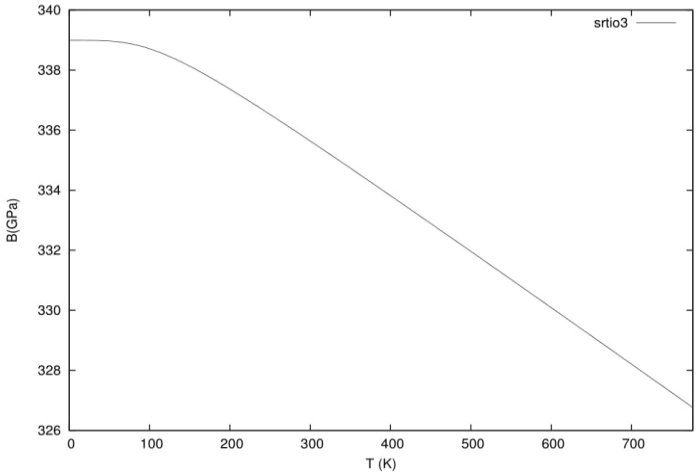

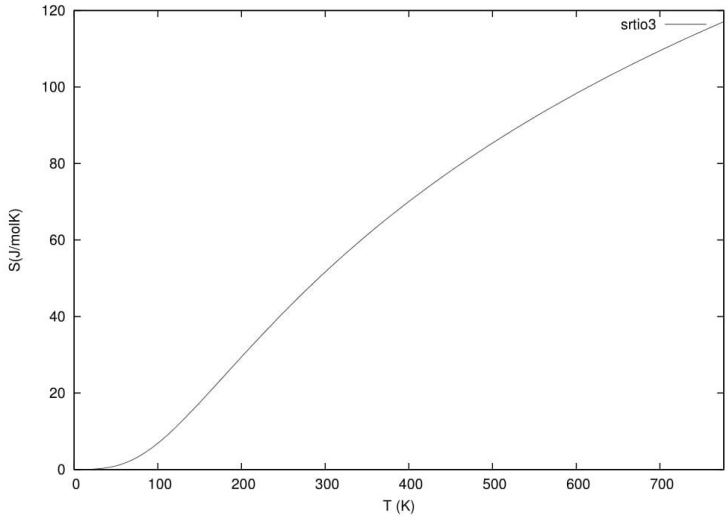

Fig 4.8 (i)Gibbs free energy, (ii)Bulk modulus and (iii)entropy vs T relation for bulk separated by layer at distance 18.897a.u

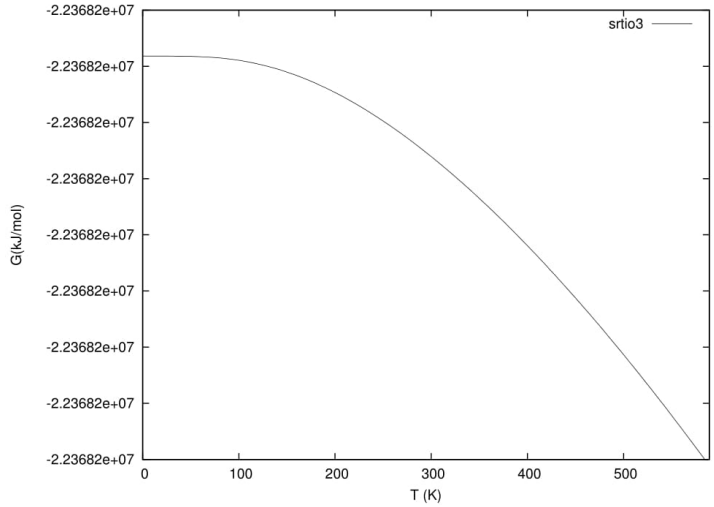

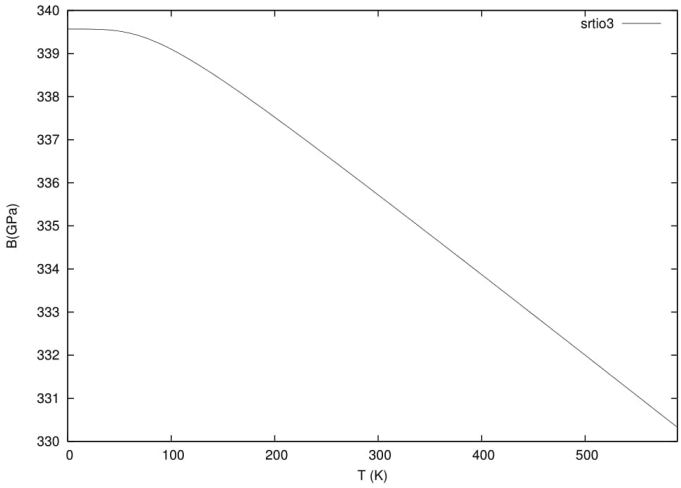

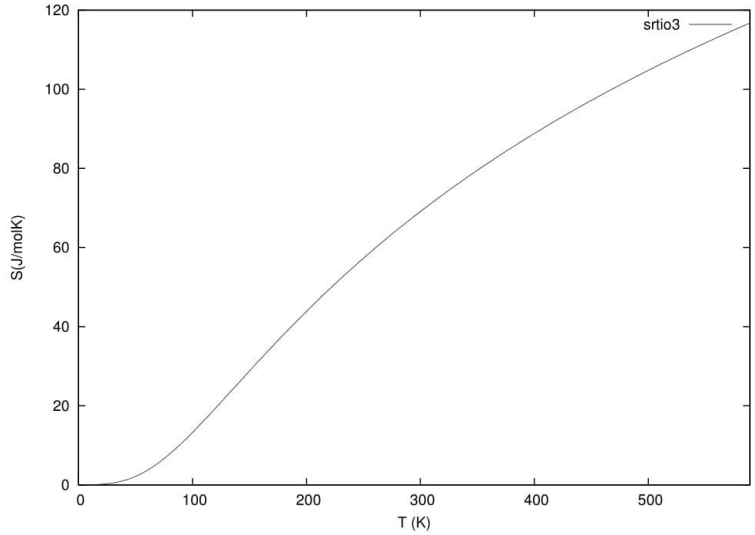

Fig 4.9 (i)Gibbs free energy, (ii)Bulk modulus and (iii)entropy vs T relation for Bulk $SrTiO_3$

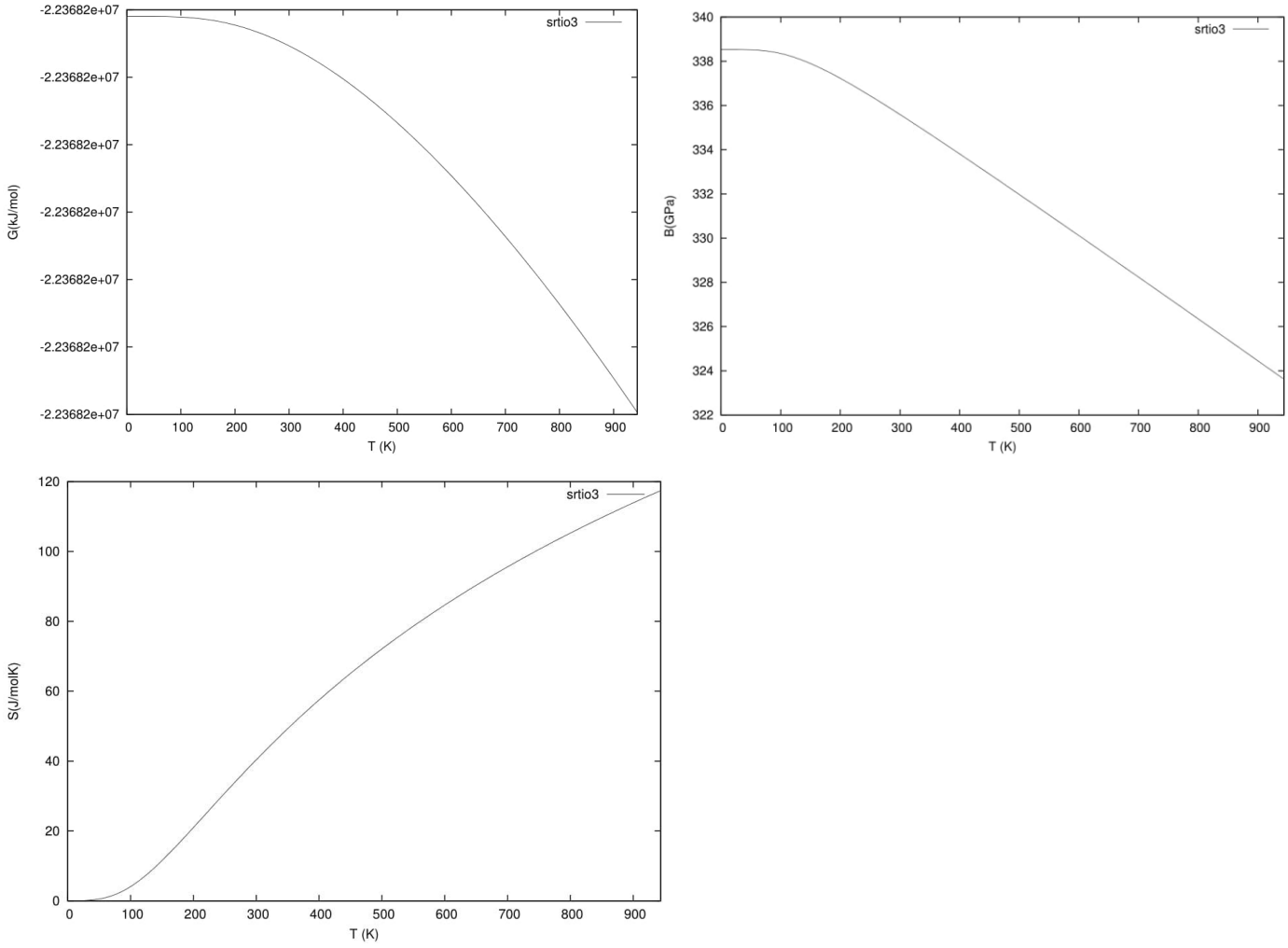

The temperature range from 0 to 1200 K, where the quasi-harmonic model is fully valid, is used to determine the thermal properties.

Using the formula G=E+PV+TS, Gibbs free energy is utilised to calculate the thermodynamic stability of the compound ce. E represents the system's internal energy, and S is its entropy. The Gibbscode2 is used to calculate the aforementioned values. Utilizing the Debye model and the Gibbs code, the thermodynamic properties are defined [22]. Fig. 4.6(i) to 4.9(i) shows the compound's Gibbs free energy vs. temperature relationship. The Gibbs energy is seen to decrease as temperature rises, indicating that the chemical is thermodynamically stable.

According to Fig. 4.6(ii) to 4.9(ii), relationships between bulk modulus at different temperatures of 0, 200, 400, 600, 800, 1000, and 1200 K, respectively, are all almost linear.Bulk modulus decreases as the temperature increases.Temperature causes a drop in the bulk modulus.

Fig 4.6(iii) to 4.9(iii) gives the entropy vs temperatue of 0-1200k, the entropy increases with increase in temperature.These properties are good in results with literature [16].

CONCLUSION

The perovskite compound namely $SrTiO_3$ with cubic structure (221_pm_3m) is studied under the Full Potential Linearized Augmented Plane Wave (FP-LAPW) method as implemented in the WIEN2K code. The analysis are made in both of its bulk and layer phases of $SrTiO_3$ structures with respect to electronic, optical and thermal properties. The density of states (DOS), band structure, and optical histograms are shown in order to represent the properties of electron and phonon transfer. The $SrTiO_3$ exhibits a semiconductor behavior in GGA approximations as evidenced by the band structure having a direct bandgap at Γ symmetry point. In the energy range of 0 to 14 eV, optical parameters like the dielectric constant, reflectivity coefficient, refractive index, optical conductivity, and energy loss function were studied. All of the values and attributes match very well with previous compared experimental and theoretical findings. From the comparative study of bulk and layered structures, layered $SrTiO_3$ materials will be more efficient materials for optical devices, In particular layered structure separated by distance 18.897eV. Especially Layered structured perovskites have titanic potential for novel device applications than reported bulk material.

Reference

[1] Gillani SSA, Ahmad R, Islah-u-din, Rizwan M, Shakil M, Rafique M, Murtaza G, Jin HB, First-principles investigation of structural, electronic, optical and thermal properties of Zinc doped $SrTiO_3$, Optik (2019), doi: https://doi.org/10.1016/j.ijleo.2019.163481

[2] Thermoelectric properties of $BaFe_2As_2$ and Ba_2FeAs_2 Compounds

July 2018 Publisher: Scholar's Press, ISBN: 978-620-2-31424-4

Project: DST-FIST, India SR/FST/PSI-193/2014 dated 23-07-2014

[3] L. Khaber, et al., Solid State Commun (2014), http://dx.doi.org/10.1016/j.ssc.2014.03.018

[4] Electronic and optical properties of bulk and surface of CsPbBr3 inorganic halide perovskite a frst principles DFT 1/2 approach Mohammed Ezzeldien1,7, SamahAl-Qaisi2 , Z.A.Alrowaili1 , MeshalAlzaid1 , E. Maskar3 , A. Es-Smairi4 , TuanV.Vu5,7 & D. P. Rai

[5] Bulk properties and electronic structure of $SrTiO_3$, $BaTiO_3$, $PbTiO_3$ perovskites: an ab initio HF/DFT study Author links open overlay panelSPiskunov[a]EHeifets[b]R.IEglitis[a]GBorstel[a]

[6] A comparative study of structural, electronic and optical properties of cubic CsPbI3: bulk and surface KUMAVAT SONI1, N LAKSHMI1, ∗, VISHAL JAIN2, AARTI RANI CHANDRA1 and RAKESH JAIN

[7] Theoretical study of Ni doping $SrTiO_3$ using a density functional theory

Z. Aboub [1,,], B. Daoudi [1,2], A. Boukraa [1] AIMS Materials Science 2020, Volume 7, Issue 6: 902-910. Doi: 10.3934/matersci.2020.6.902

[8] Xiang Liu & Karl Sohlberg (2014) Theoretical calculations on layered perovskites: implications for photocatalysis, Complex Metals: An Open Access Journal, 1:1, 103-121 DOI: 10.1080/2164232X.2014.891950.

[9] S.A. Khandy, D.C. Gupta, Electronic Structure, Magnetism and Thermoelectricity in Layered Perovskites: Sr2SnMnO6 and Sr2SnFeO6, Journal of Magnetism and Magnetic Materials (2017), doi: http:// dx.doi.org/10.1016/j.jmmm.2017.05.058

[10] Bulk electronic structure of $SrTiO_3$: Experiment and theory K. van Benthema) and

C. Elsa¨sser Max-Planck-Institut fu¨r Metallforschung, Seestrasse 92, D-70174 Stuttgart, Germany R. H. French DuPont Corporation Central Research, E356-384, Exp. Street, Wilmington, Delaware 19880-0356.

[11] DOI: 10.17188/1263154

[12] The electronic structures and optical properties of BaTiO3 and $SrTiO_3$ using first-principles calculations C.B. Samantaray*, Hyunjun Sim, Hyunsang Hwang.

[13] Electronic Structure Basis for Enhanced Overall Water Splitting Photocatalysis with Aluminum Doped $SrTiO_3$ in Natural Sunlight Zeqiong Zhao,a Renato V. Goncalves,a,b Sajib K. Barman,c Emma J. Willard,a Edaan Byle,a Russell Perry,a Zongkai Wu,a Muhammad N. Huda,*c Adam J. Moulé,d and Frank E. Osterloh*a

[14] G. Cappellini, S. Bouette-Russo, B. Amadon, C. Noguera, and F. Finocchi, J. Phys.: Condens. Matter 12, 3671 ~2000!

[15] Structural, Electronic and Optical Properties of Copper-doped SrTiO Perovskite: 3 A DFT Study Muhammad Rizwan, Adnan Ali, Zahid Usman, N.R. Khalid, H.B. Jin, C.B. Cao

[16] A. Boudali; M. Driss Khodja; B. Amrani; D. Bourbie; K. Amara; A. Abada (2009). *First-principles study of structural, elastic, electronic, and thermal properties of $SrTiO_3$ perovskite cubic., 373(8-9), 879–884.* doi: 10.1016/j.physleta.2008.12.017

[17] S. Piskunov, E. Heifets, R.I. Eglitis, G. Borstel, Comput. Mater. Sci. 29 (2004) 165.

[18] J. Robertson, K. Xiong, S.J. Clark, Thin Solid Films 496 (2006) 1.

[19] E. Mete, R. Shaltaf, S. Ellialtıoglu, Phys. Rev. B 68 (2003) 035119

[20]O. L. Anderson, **J. Phys. Chem**. Solid 24 909 (1963).

[21] E. Heifets, E. Kotomin, V.A. Trepakov, J. Phys.: Condens. Matter 18 (2006) 4845.

[22] Jayalakshmi D S, Sundareswari M, Viswanathan E, Hemanand D and Venkat Pranesh 2019 Int. J. Modern Physics B 33 1950341

[23]https://www.sciencedirect.com/science/article/pii/B012226770203951X R. Mokaya,in Encyclopedia of Separation Science, 2000.

[24] https://doi.org/10.1039/1364-5501/1991, Themed issue: layered materials: structure andproperties.

[25] R. G Parr and W.Yang, Density Functional Theory of Atoms and Molecules(Oxford, Oxford,1989).

[26] Samrana Kazim, Mohammad Khaja Nazeeruddin, Michael Gr¨atzel, and Shahzada Ahmad. Perovskite as light harvester: a game changer in photovoltaics. Angewandte Chemie International Edition, 53(11):2812–2824, 2014

[27]KP Rajeev, GV Shivashankar, and AK Raychaudhuri. Low-temperature electronic properties of a normal conducting perovskite oxide (lanio3). Solid state communications, 79(7):591–595, 199.

[28] P. Blaha, K. Schwarz, P. I. Sorantin and S. B. Tricky, Full-potential linearinsed augmented plane wave programs for crystalline systems, Computer. Phys. Commun., 59, (1990) 399- 415.

[29] D.S. Jayalakshmi and M. Sundareswari, Indian journal of Physics 89 (2015) 201-208

[30]Schwarz K. Blaha P. Comp.Phys.Comm.147, 71-76(2002)